POLITECNICO DI TORINO
Repository ISTITUZIONALE

Comparative Analysis of Electric Vehicle Simulator for Accurate Battery Pack Internal Signal Generation

Terms of use:

(Article begins on next page)

22 December 2024

Comparative Analysis of Electric Vehicle Simulator for Accurate Battery Pack Internal Signal Generation

Raimondo Gallo, Tommaso Monopoli, Marco Zampolli, Rémi Jaboeuf, Paolo Tosco,
Alessandro Aliberti, and Edoardo Patti

Abstract—The definition of accurate electric vehicle (EV) simulators can help mitigate the lack of large-scale public battery pack datasets in literature. This work compares two developed Simulink-based EV simulators that generate realistic EV battery pack signals from input driving sessions. The two EV simulators, referred to as simplified and advanced respectively, share the same architecture. However, they are equipped with internal blocks characterized by different complexity and precision. Both simulators generate time series of the vehicle's speed, and battery pack's current, state of charge (SOC), voltage, and internal temperature. Additionally, the simulators incorporate thermal and aging models, allowing for the emulation of a wide range of environmental conditions and aging statuses of the battery pack. A subset of inner parameters has been set, sourcing from online technical data sheets, to enable both virtual-EVs to mimic the same 2017 Volkswagen eGolf EV model. Indeed, given the availability of an acquired and ample real dataset specific to the same EV model, it is possible to perform an extensive and thorough validation of the simulated data. Both virtual-EVs prove to be accurate at simulating a battery pack under different aging conditions, although the comparison highlights the benefits of more sophisticated design choices, demonstrating the higher accuracy of the advanced virtual-EV over the simplified one. Indeed, the advanced virtual-EV achieves overall RMSE and R^2 values, for current, voltage, and SOC of 43.34 A, 4.07 V, 4.84% and 0.28, 0.93, and 0.96, respectively. The main design differences between the two virtual-EVs are presented, and, upon examining their computational burden, distinct utilization scenarios are proposed based on the user's needs.

Index Terms—Electric vehicle, Battery pack, Simulation, Matlab, Simulink

NOMENCLATURE	
BOL	Beginning-of-Life
DC	Driving Cycle
DOF	Degree of Freedom
EFC	Equivalent Full Cycles
EOL	End-of-Life
EV	Electric Vehicle
HEV	Hybrid Electric Vehicle
LIB	Lithium-ion Battery
ML	Machine Learning
OCV	Open-Circuit Voltage
$R0$	Terminal Resistance
$RMSE$	Root Mean Squared Error
R^2	Coefficient of Determination
SOC	State of Charge
SOH	State of Health

R. Gallo, T. Monopoli, A. Aliberti and E. Patti are with Politecnico di Torino, Torino, Italy (e-mail: name.surname@polito.it).

M. Zampolli, R. Jaboeuf, P. Tosco are with Edison S.p.A., Milano, Italy (e-mail: name.surname@edison.it).

I. INTRODUCTION

One of the most important challenges of this century is thought to be climate change mitigation. According to estimates, the transportation industry is responsible for 27% of all greenhouse gas emissions in the world. More precisely, road travel is responsible for 75% of all CO_2 emissions in the transportation sector [1]. Both in the private and public transportation sectors, EVs have received widespread acceptance as a dependable and clean substitute for conventional vehicles, and it is expected that they will soon take over the market in the future years [2]. Investigating novel technologies that can improve EV performance is crucial.

The battery pack, which is the essential element of an EV, is normally constructed from many battery cells linked in parallel and in series. Due to their numerous advantageous characteristics, the cells composing a lithium-ion battery (LIB) are currently the most crucial technology in battery pack design [3]–[5]. Due to a variety of chemical and mechanical changes to the electrodes during time and operation, LIB cells, like other batteries, are susceptible to degradation events. It is crucial to analyze the EV battery pack to grasp the basics of its health condition and lifespan. Data-driven procedures, such as machine learning (ML) approaches, can produce state-of-the-art achievements in many disciplines, given the capacity of such models to resolve non-linear issues. Indeed, academia and business have recently shown significant interest in developing novel methods for measuring the performance of EVs by integrating ML algorithms, such as predicting LIB performances [6] or spotting battery failure signs [7].

Nonetheless, in order to adopt data-driven procedures, huge amounts of measurements are required. Unfortunately, the data that are available are either scarce or challenging to retrieve. Users can access a few open battery datasets [8] [9], but they include monitoring information gathered from lab tests performed on a single cell or a small group of cells, which cannot accurately reflect an EV battery pack as a whole. Several private EV fleet management companies, through onboard diagnostic tools, can gather a substantial quantity of battery pack data. But such data are either inaccessible or sold at a very high price. Thus, it becomes quite challenging obtaining large-scale and open datasets of actual EV monitoring data [10] to investigate and improve EV technologies. Hence, the definition of EV simulators would enable the generation of synthetic data for the full battery pack, filling the data

availability gap. This would allow researchers to train the suggested ML models using EV-simulated data, enabling them to create new data-driven methods for monitoring the EV's battery pack.

In previous works [11] [12], two EV model simulators have been developed, which are referred to as simplified and advanced virtual-EVs, respectively. Both mimic the same specific real-world EV model, a 2017 Volkswagen eGolf, and are designed using MATLAB and Simulink programing frameworks. The two virtual-EVs reproduce an entire EV system made up of numerous mutually dependent subsystems, such as an electric motor, battery pack, wheels, and braking system, enabling the generation of battery pack signals, taking into account complex interactions among all subsystems. The simplified and advanced simulators share the same architecture in terms of blocks, although some of the inner blocks implement the EV subsystems with different levels of precision and realism. Indeed, as the name suggests, the advanced EV simulator improves several aspects of the simplified one related to the motor and battery blocks, the vehicle body, the thermal and aging models embedded in the battery pack, the inclusion of customizable wind resistance, and overall contribution of onboard auxiliary devices. Both EV simulators generate synthetic time series of speed, battery current, voltage, state of charge (SOC), and internal temperature.

In this work, an exhaustive comparison of the two virtual-EVs is carried out, analyzing the main different design choices. Moreover, a thorough validation of the simulation results is achieved utilizing data from actual driving sessions. The real EV data have been collected from the same real-world EV model, mimicked by both virtual-EVs, throughout its lifespan, hence characterized by different aging conditions of the battery pack, with its state of health (SOH) ranging from 85% to 99%. Indeed, the EV battery pack's SOH generally ranges from 100%, corresponding to a brand-new battery at the beginning-of-life (BOL), to 80% at the end-of-life (EOL) when the battery must be replaced. Given the heterogeneity of the acquired actual data, covering almost entirely the lifespan of the battery pack, it becomes possible to precisely determine the accuracy of both virtual-EVs in different environmental and internal conditions.

Firstly, sourcing from online technical data sheets specific for the selected 2017 Volkswagen eGolf EV model, a subset of the blocks' inner parameters has been tuned to optimally represent the actual operations of the chosen real-world EV. Then, the synthetic outputs from both simplified and advanced virtual-EVs are independently validated by utilizing the acquired actual signals. The modularity of the proposed virtual-EVs, along with the possibility to freely tune the blocks' parameters, allows the emulation of, potentially, a vast variety of EV models.

Both virtual-EV can be utilized to generate accurate and realistic EV battery datasets, enriching the selection of the data collections available in literature. Moreover, the comparison of the simulated data demonstrates the overall higher precision of the advanced virtual-EV over the simplified one, at the cost of a greater computational burden. Nonetheless, considering the trade-off between precision and complexity of the two simulators, it is advised the employment of the simplified virtual-EV to simulate EVs, seen as floating batteries, in a collective and large scenario, fastening the retrieval of the results with a lower precision. Conversely, the advanced virtual-EV could be utilized to precisely simulate individual EVs, collecting more accurate outputs at the expense of faster data retrieval.

The rest of this paper is structured as follows. Section II provides a general outlook of the available EV simulators in the literature, and their characteristics; while, Section III provides a detailed description of the proposed simplified and advanced virtual-EVs structure, design differences, and required inputs and outputs. Section IV discusses the experimental results. Finally, Section V provides concluding remarks and plans for further research.

II. RELATED WORK

Numerous studies in literature focus on enhancing EV performance monitoring with ML. However, in order to use data-driven approaches, substantial and detailed datasets are required. Therefore, by defining EV simulators, it may be possible to gather enough data to provide ML algorithms with input.

Large-scale EV modeling and simulation has undergone significant work in order to analyze the load exchanged between EVs and the power grid. Indeed, Canizes et al. [13] created a travel simulation application that simulates an actual environment, including trips and charging stations to build customized profiles, itineraries, and schedules, considering the behavior of real users. The technology being used focuses on how changes in energy pricing affect how EV customers behave, emphasizing that consumers benefit more from variable-rate electricity prices. A Java-based tool called EVLibSim, proposed by Rigas et al. [14], enables simulation of EV operations at the level of charging stations in a smart grid setting. A charging station can be designed using EVLibSim, an event-based simulation framework, based on the needs of the user. In this way, EV queues charges and discharges can all be precisely simulated. Emobpy is an open-source Python tool developed by Gaete-Morales et al. [15] that generates EV time series sourcing from 200 input vehicle profiles in Germany. Emobpy provides four output time series with adjustable length and resolution based on empirical mobility statistics and physical features of vehicles. The output time series contain data on vehicle mobility, driving electricity consumption, grid availability, and grid demand. Large EV fleets can be monitored using the simulation tool, which also provides essential inputs for energy, environmental and economic applications.

The availability of EV-to-Grid simulators helps understand the impact of large EV fleet over the electrical grid, allowing to suggest the best charging strategies minimizing the peak load required by the EVs. On the other hand, being able to simulate the internal behavior of an EV's battery pack would help the investigation of novel techniques to improve the EV technologies.

Ciabattoni et al. [16] developed an entirely programmable event-based simulator that can generate plug-in/out, charge,

and discharge events for a collection of EVs or a single EV. To increase the tool's functionality and enable integration into different applications, it is developed as a web simulator called ePopSimulator and a Matlab/Simulink block. The simulator's ability to enable users to change the simulation scenario and receive both aggregated and individual EV statistics makes it perfect for researching vehicle-to-grid solutions. FASTSim is an open-source vehicle simulation tool developed by Brooker et al. [17] that can design both conventional and electric automobiles. It accurately models vehicle parts while retaining high accuracy, which is made possible by validating the results using information from numerous cars. Researchers can use the tool to investigate ways to enhance EV technology, including the estimation of energy use.

For other scenarios, it is instead useful simulating inner the battery pack of an EV, along with its other subsystems, to investigate how the involved technologies impact on efficiency and driving experience of the vehicle. Lee et al. [18] modeled a lithium-polymer battery pack utilizing the Advanced Light-Duty Powertrain and Hybrid Analysis (ALPHA), created by EPA, along with its thermal model and typical hybrid electric vehicle (HEV) BMS cooling strategies. The battery simulator generates output signals of voltage, current, SOC, and temperature, which are validated using reference real EV data achieving a voltage error of 2.2V

Hanifah et al. [19] developed an EV system, including a simple battery system, to investigate the different battery technologies in EV achieving the best travel range. Comparing the output SOC and vehicle range, they demonstrated that LIB allow to cover higher distances due to their higher energy density. Hederić et al. [20] proposed an EV simulator in Matlab/Simulink, parameterized with actual data retrieved from the catalogue of the mimicked EV manufacturer. The simulation results highlight the dynamic characteristics of the modeled LIB for distinct standardized charge and discharge regimes. Kroeze et al. [21] programmed a Matlab/Simulink battery model predicting SOC, terminal voltage, and power losses. After a careful tuning of the parameters, accomplished through laboratory tests, they tested the battery model in a plug-in HEV simulator, verifying the accuracy of the simulated outputs.

Qin et al. [22] developed a Modelica LiFePO$_4$ battery pack tuned through experiments conducted over a real battery. Given the input current, the output voltage achieves a maximum error of 1.78%. The battery model was then coupled with a Modelica EV simulator which can accurately estimate the driving mileage. Simic et al. [23] built a HEV model, using Modelica packages, featuring an ideal battery pack. Using accessible measurements and data sheets, they parameterized the EV model and used the actual measured current as a reference signal. The battery voltage validation shows a 5% difference between the observed and simulated data. Shin et al. [24] presented a vehicular LIB parameterized utilizing data collected through a chassis dynamometer test. They tested different battery models obtained by scaling up and down the cell and battery parameters, respectively. The battery models are then applied to EV model simulation proving comparable levels of accuracy.

Table I reports a summary of the discussed works, with their main characteristics, simulating the inner behavior of the battery pack, also in a vehicular context. Particularly, Table I includes information regarding the modeled system, the simulator's inputs, environmental inputs, and outputs, the output granularity (if specified), and whether the impact of the battery aging is investigated from the simulation outputs. It is also reported whether the results have been validated with real data and, finally, the numeric performances achieved.

The proposed scientific novelty in this work includes a thorough comparison between the two developed virtual-EVs [11] [12], starting from the general description of the two simulators' main design differences, highlighting the improvements introduced by the advanced virtual-EV over the simplified one. Through the specification of a set of inputs, both EV simulators produce output signals for the battery pack's current, voltage, SOC, and internal temperature. The possibility of specifying environmental inputs, such as road slope, wind resistance, and external temperature, makes the simulated data closer to a realistic scenario.

Observing Table I and comparing the proposed simulators with those in literature, this work evaluates the accuracy of the virtual-EVs comparing their outputs with actual benchmark data collected from battery packs, within the same mimicked real-world EV, at different aging conditions. Indeed, thanks to the higher availability of reference data, it is possible to extensively analyze the performances of the proposed simulators considering the battery aging and the effect of environmental factors acting over the modeled EV.

Although sharing the same general modular structure, the comparison highlights the higher precision of the advanced virtual-EV with respect to the simplified one, justifying the more sophisticated adopted design choices. Indeed, the advanced virtual-EV reduces the overall RMSE for voltage and SOC by 5.23 V and 7.60%, respectively. As demonstrated, both simulators achieve low errors for different aging conditions of the battery pack, making the virtual-EVs robust for a wide range of environmental and internal conditions.

By sourcing from online specific and technical data sheets, it is possible to parameterize the inner block of the simulators mimicking, potentially, any EV model of interest. With the employment of the advanced virtual-EV, the user could generate synthetic and realistic signals of internal battery pack signals. In this way, the user could do without time-consuming laboratory experiments or costly devices collecting data from the EV's battery management system. The generation of realistic and accurate battery EV data enables the development of data-driven ML techniques to conduct in-depth research on battery performances. Conversely, the user could utilize the simplified virtual-EV, for instance, to create a fleet of EVs, seen as floating batteries, to propose charging strategies in a large urban scenario.

III. MATERIALS AND METHODOLOGY

This section presents the general and common inner structures of the simplified and advanced virtual-EVs, highlighting their differences which will, inevitably, lead to different

TABLE I
THE SUMMARY OF SIMULATORS IN LITERATURE WITH THEIR MAIN CHARACTERISTICS, MODELING EITHER THE BATTERY PACK ALONE OR IN A FULL EV ENVIRONMENT.

| Authors	Modeled system	Inputs	Environmental inputs	Outputs	Output granularity [s]	Aging analysis	# real sessions	Performance
Lee et al. [18]	Battery pack	Technical parameters	✗	Battery's voltages, currents, SOC, internal temperature	✗	✗	3	Battery voltage RMS 2V
Hanifah et al. [19]	Battery pack + EV system	Technical parameters	✗	Battery's voltage, current, EV's range and speed	✗	✗	✗	✗
Hederic et al. [20]	Battery pack + EV system	Technical parameters, speed	Rolling resistance, air resistance	Battery's voltage, current, SOC, EV's speed and motor power	✗	✗	✗	✗
Kroeze et al. [21]	Battery pack + EV system	Technical parameters, speed	✗	Battery's voltage, current, power response	✗	✗	1	Battery terminal voltage 0.199% SOC 1.00%
Qin et al. [22]	Battery pack + EV system	Technical parameters, speed	Rolling resistance, air resistance	Battery's voltage, current, SOC, EV's mileage	✗	✗	1	Battery voltage 1.78% EV mileage 0.54%
Simic et al. [23]	Battery pack + HEV system	Technical parameters, current	Rolling resistance, air resistance	Battery's voltage	✗	✗	1	Battery voltage lower than 5%
Shin et al. [24]	Battery pack + EV system	Technical parameters, speed	Rolling resistance	Battery's voltage, current, SOC, EV's speed, motor RPM and torque	✗	✗	2	Battery voltage RMSE 3.93V (at high SOC) RMSE 2.27V (at low SOC)
Proposed simplified virtual-EV	Battery pack + EV system	Technical parameters, speed	Rolling resistance, air resistance, road slope, environmental temperature	Battery's voltage, current, SOC, internal temperature	0.2	✓	23	Overall battery current R^2 0.26 voltage R^2 0.65 SOC R^2 0.75 internal temp. R^2 0.95
Proposed advanced virtual-EV	Battery pack + EV system	Technical parameters, speed	Rolling resistance, air resistance, road slope, environmental temperature	Battery's voltage, current, SOC, internal temperature	0.1	✓	23	Overall battery current R^2 0.28 voltage R^2 0.93 SOC R^2 0.96 internal temp. R^2 0.97
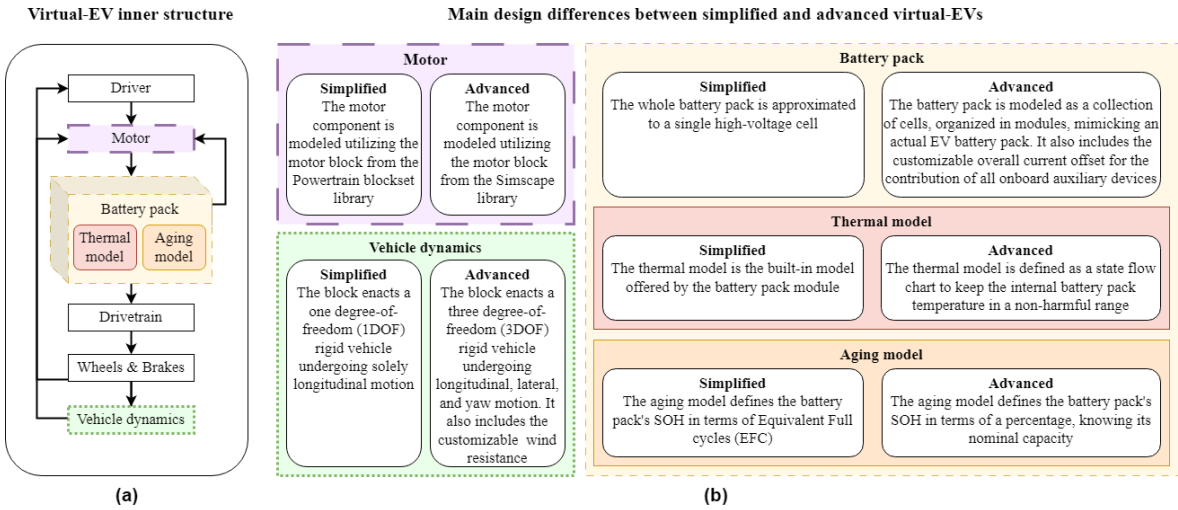
Fig. 1. (a) General and common inner structure of the simplified and advanced virtual-EVs. (b) The description of the two virtual-EVs' main design differences.

levels of accuracy and precision of their synthetic outputs. Finally, the required simulation inputs and the characteristics of the generated synthetic internal battery pack's signals are discussed.

A. Dataset

The employed dataset consists of actual data gathered during 23 distinct real driving sessions from EVs belonging to the same 2017 Volkswagen eGolf model. A driving session refers to information related to the user's driving experience, including time series of: vehicle's speed [km/h], battery's voltage [V], current [A], internal and environmental temperatures [°C], and SOC [%]. The internal temperature refers to the global inner temperature of the battery pack; while the environmental temperature corresponds to the outdoor one, which has an impact on the battery pack's internal temperature. The real data are utilized to tune a subset of the simplified virtual-EV's parameters and to validate the performances of both virtual-EVs independently. Each real driving session, at the time data was collected, is characterized by different internal and environmental conditions, such as the initial SOH of the battery pack and outside temperature.

Indeed, thanks to the variability of the battery pack's SOH for the available driving sessions, it is possible to analyze the simulators' performance throughout almost the full lifespan of the EV's battery pack, ranging from 85% to 99%, close to the battery lifespan extremes, BOL and EOL. Hence, with the data at disposal, the accuracy of the simplified and advanced simulators can be quantified in different driving conditions, accounting also for distinct aging statuses of the battery pack.

In Table II, reports the description of the available real driving sessions, with their main distinctive traits. Throughout the manuscript, the terms driving session and Driving Cycle (DC) are used interchangeably, although DC refers to the simulators' inputs, including the speed time series, to which the EV was subjected, along with other internal and environmental conditions.

Additionally, the onboard device, gathering the actual signals, samples the data at different sampling frequencies. The original sample frequency for each signal acquired from the real-world EVs is reported in Table III. The real data are independently resampled using linear interpolation, with a common frequency matching the output one of the virtual-EVs, that is 0.2 and 0.1 seconds for the simplified and advanced simulators, respectively, as also discussed in Sec-

TABLE II
THE AVAILABLE REAL-WORLD EVs DRIVING SESSIONS ALONG WITH
THEIR MAIN CHARACTERISTICS.

Driving cycle	SOH [%]	Duration [s]	Avg. speed [km/h]	Avg. SOC [%]	Environmental temp. [°C]
DC1	85	10606	41.16	61.98	-2.33
DC2	85	9333	41.86	41.95	1.12
DC3	85	7575	20.19	77.49	2.70
DC4	88	10639	63.07	58.04	-0.63
DC5	88	9124	34.09	76.55	9.06
DC6	88	17130	28.58	60.10	8.49
DC7	92	4374	49.52	85.09	15.65
DC8	92	8899	50.77	29.79	24.86
DC9	93	6089	67.01	81.82	20.04
DC10	93	2418	48.90	21.87	30.38
DC11	93	16431	37.30	49.71	24.03
DC12	94	3461	31.32	31.25	0.09
DC13	94	4584	97.75	53.49	10.03
DC14	94	4249	60.57	78.16	19.78
DC15	95	3039	58.03	84.21	17.60
DC16	95	1591	49.34	49.08	12.40
DC17	95	313	30.71	91.85	1.00
DC18	96	3045	46.71	81.63	15.29
DC19	96	3063	87.09	48.74	14.20
DC20	98	2198	86.24	60.25	31.14
DC21	99	3510	20.26	92.77	22.75
DC22	99	4919	44.21	76.04	20.82
DC23	99	8570	36.04	38.76	17.78

tion III-B2. Such a resampling ensures consistency across real and synthetic signals, allowing the correct validation of the simulation results. A fast sampling rate may capture high-frequency changes in the signals more precisely but at the expense of a longer simulation time. The choice of sampling rate consists of a trade-off between computing time and the quality of the signal.

B. The virtual-EV

The main focus of this work is to present a virtual-EV model simulator to generate accurate battery pack's current, voltage, internal temperature, and SOC signals, allowing the monitoring of battery conditions throughout the EV's operational time. As a result, the battery pack becomes the most important virtual-EV's component. In fact, the lack of specific internal design parameters in the literature makes modeling an EV battery pack challenging. Figure 1 (a) shows the schematization of the inner structure of the simulator, shared by both simplified and advanced virtual-EVs. While, Figure 1 (b), describes the main high-level design differences block by block between the two simulators, although exhaustively discussed later on in this same section.

1) The general inner structure: The virtual-EV is defined as several mutually dependent subsystems interconnected to each other, mimicking the operations of an actual EV. Particularly, the same *Driver*, *Drivetrain*, *Wheels and Brakes* blocks are shared between simplified and advanced virtual-EVs; while the implementation of the *Motor*, *Battery pack*, and *Vehicle dynamics* blocks is different, and they contribute to the higher precision of the advanced simulator over the simplified one. Specifically, the *Driver* block implements a discrete-time

TABLE III
THE SAMPLING RATES OF THE COLLECTED REAL SIGNALS.

Data signal	Sampling rate [s]
Speed	19
Current	0.1
Voltage	0.1
SOC	11
Internal temperature	41
Environmental temperature	110

proportional-integral controller that simulates a human driver for the car. The controller attempts to match the simulated vehicle speed, at each time step, with the input reference DC speed signal by operating on the brake and accelerator pedals. The *Drivetrain* block, belonging to the Powertrain Blockset [25], consists of a complex arrangement of rotating shafts, gears, and other components that work together to efficiently and effectively distribute power. Hence, it plays a crucial role in transmitting the mechanical power generated by the electric motor to the wheels, allowing the vehicle to move.

The *Wheels and Brakes* block, implemented using the Longitudinal Wheel with Disc Brake Simulink block provided by Powertrain Blockset library [26], represents the behavior of the wheels and the braking system, which incorporates the friction braking and regenerative braking. The former is the standard braking system that is activated by applying pressure to the brake pad, creating friction force that is opposed to the wheel's direction; the latter, while slowing down the vehicle, recharges the EV's battery pack. The *Motor* block enacts a mathematical representation of an electric motor running in torque control mode. The *Battery pack* block represents the EV's battery subsystem, and it embeds thermal and aging models to further characterize the synthetic driven session and to improve the quality of the virtual-EV's output signals. Finally, the *Vehicle dynamics* block simulates the longitudinal motion of a vehicle's body, and it takes into account various forced and factors affecting the vehicle's motion, such as the wind resistance and road slope.

The detailed list of the parameters specific to the mimicked reference EV model and utilized to parameterize the main blocks of the two virtual-EVs is reported in Table IV.

TABLE IV
DETAILED INFORMATION FOR BATTERY, MOTOR, AND VEHICLE
BELONGING TO THE MIMICKED 2017 VOLKSWAGEN EGOLF EV MODEL.

	Description	Value
Battery pack	Type	Lithium-ion
	Capacity [kWh]	35.8
	Voltage [V]	323
	Number of cells	264
	Number of modules	24
	Cell weight [kg]	0.692
Motor	Type	Synchronous AC Permanent Magnet
	Maximum torque [lb-ft]	214
Vehicle	Drag Coefficient	0.27
	Curb Weight [kg]	1567
	Gross Vehicle Weight [kg]	2010
	Frontal area [m^2]	2.19
	Wheels radius [m]	0.26
	Tire rolling resistance	0.01

2) Simplified Vs advanced virtual-EVs: Since, as previously described, the *Driver*, *Drivetrain*, *Wheels and Brakes* blocks are shared between simplified and advanced virtual-EVs, the main differences between the two simulators lie on the design and implementation of the *Motor*, *Battery pack* (along with its thermal and aging models), and *Vehicle dynamics* blocks. Referring to Figure 1 (b), the *Motor* block is implemented using the Simulink Mapped Motor [27] and the Simscape library [28] for the simplified and advanced simulators, respectively. Although belonging to distinct libraries, both blocks implement an electric motor operated in torque-control mode. However, the motor block within the advanced virtual-EV, directly connected to the thermal model, allows the modelling of losses converting power to heat, making it more accurate.

The *Vehicle dynamics* block within the simplified virtual-EV represents the vehicle body as a one degree-of-freedom (1DOF) rigid body with constant mass, solely undergoing longitudinal dynamics, and it is implemented using the Vehicle Body 1DOF Longitudinal Simulink block [29]. Conversely, in the advanced virtual-EV, such a block defines the vehicle body as a three degree-of-freedom (3DOF) rigid body with constant mass undergoing longitudinal, vertical, and pitch motion, and it is modeled with the Vehicle Body 3DOF Longitudinal block [30]. Also, in contraposition to the simplified virtual-EV, through the *Vehicle dynamics* block within the advanced virtual-EV, a constant longitudinal wind resistance of 4 m/s is imposed, although customizable by the user, with the intention of generating more realistic output signals.

The main core difference between simplified and advanced virtual-EVs lies on the definition of the battery pack sub-system. Indeed, in the simplified simulator, the battery pack is modeled using the Generic Battery Model (GBM) block from the Simscape electrical Simulink library [31], and it is approximated to a single high-voltage cell. The simplified battery pack, as reported in Figure 1 (b), embeds a thermal model that describes the discharge characteristics at a second operating condition (different from the nominal one), characterized by a chosen environmental temperature. Moreover, battery-to-ambient thermal interaction is described by the two parameters, thermal resistance and thermal time constant.

The GBM block features a simple aging model of the battery, which is described by a set of parameters including the battery age, defined as number of Equivalent Full Cycles (EFC), which characterizes the battery pack's aging throughout the simulation. A virtual cycle of the battery's charge and discharge is referred to as an EFC, and it occurs at a specific depth of discharge (usually, Depth of Discharge (DOD) = 100%, meaning a full charge and complete discharge).

Due to the unavailability of a specific data sheet, the set of parameters describing the battery pack's aging model of the simplified virtual-EV has been discovered through an iterative procedure that minimized the error between simulated and real battery signals [11]. Also, a linear relationship between EFC and SOH, depicted in Figure 2, arose through few conducted experiments over the Simulink's generic battery model, which allows the user to easily specify the battery pack's aging in terms of EFC, knowing its corresponding SOH percentage values [11]. The finding reveals the relationship between EFC and SOH for the Simulink's generic battery model to be linear, although for real batteries such a relation is generally not linear. Finally, the simplified virtual-EV generates output battery signals with a sampling frequency of 0.2 seconds.

Conversely, the advanced virtual-EV embeds a battery pack defined as multi-cell subsystem, sourced from Simscape Battery library [32], replicating the structure of a real EV battery pack. Indeed, it consists of individual cells organized into modules and connected in series and parallel, as shown in Figure 3, mirroring the actual configuration of an EV battery pack. The output battery's current, SOC, and internal temperature are obtained averaging the outputs of the individual cells; while, the aggregated voltage corresponds to the sum of the individual cell voltages.
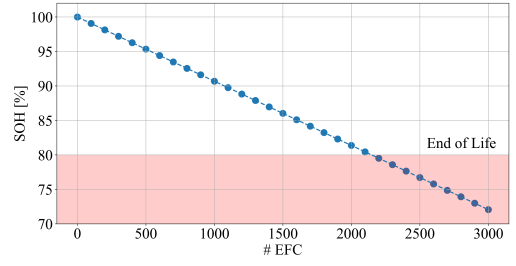

Fig. 2. The assessed linear relationship between EFC and SOH [%].

Also, the advanced simulator allows the definition of a constant current offset customizable by the user, modeling the contribution of auxiliary devices onboard the EV, which is totally missing in the simplified virtual-EV. However, the available real and target currents already embed the contribution of possible auxiliary devices. Hence, for the sake of the simulator's results validation, the current offset is set to 0 A avoiding an additional, and superfluous, contribution of the auxiliary devices.

Then, a thermal model, defined as a state flow chart and shown in Figure 4, has been added to the advanced battery pack, which acts as a thermal cooler management model, computing the heat to be released in the environment. The current value of the battery's internal temperature $Batt.\ temp$ is utilized as condition for state transitions from and into source and destination states T, respectively. The heat is computed utilizing, referring to Figure 4, the instant current i and voltage $volt$, and scalar coefficients weighting the amount of heat to be exchanged according to the current internal temperature. Indeed, the higher is the temperature, the higher is the heat to be exchanged. In this way, the battery pack's internal temperature lies within the range 25°C and 45°C, which is the realistic operational range of temperature for the battery [33]. The thermal model coefficients, i.e., 0, 0.005, 0.01, 0.025, and 0.1, utilized to compute the heat, and the state transitions $Batt.\ temp$ values, i.e., 32, 33, 34, 35, 36.5, 37, 38, and 40, as reported in Figure 4, have been discovered after a few trial-and-error tests, minimizing the overall error of the simulations' outputs.

The aging model of the advanced battery pack sets its initial aging conditions employing the following equation:

$$SOH = \frac{C_{actual}}{C_{nominal}} \tag{1}$$

where, SOH is the desired input aging status, expressed as a percentage, $C_{nominal}$ is the nominal capacity of the battery pack, retrieved from online technical data sheets specific to the modeled real-world EV, and C_{actual} is the actual and current capacity of the battery pack. In this way, a 1% decrease in
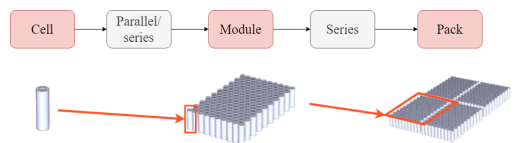

Fig. 3. The hierarchical structure of an EV battery pack [34].

SOH results in a 1% reduction in the nominal capacity. This relationship allows us to calculate the actual capacity, which is then assigned to the battery pack subsystem in the EV simulator at the beginning of the simulation.

The thermal and aging models included in the advanced virtual-EV, however, remain separate. Indeed, the capacity fading of the battery pack is solely managed by the battery pack block. However, the thermal model, depicted in Figure 4, requires the ongoing current and voltage, provided by the battery block to compute the heat to be exchanged.

Moreover, two parameters for each battery cell, namely the terminal resistance (R0) [mΩ] and open-circuit voltage (OCV) [V], have been set to further improve the characterization of the battery pack's aging status. Following the available documentation [35], the R0 and OCV parameters have been defined as matrices with dimension 7×3, and each element of the matrix corresponds to a value for a specific SOC within the range [0, 10, 25, 50, 75, 90, 100]% (rows) and temperature in [278, 293, 313]K (columns). Given the current values of SOC and internal temperature during the simulation, the values of R0 and OCV change accordingly, interpolating within the corresponding matrix. The reference element values of the two R0 and OCV matrices have been modified after a few trial-and-error tests, and their final form is reported below:

$$R0 = \begin{bmatrix} 2.6100 & 1.8961 & 2.0077 \\ 2.4538 & 1.8961 & 2.0077 \\ 2.5430 & 1.9407 & 2.0523 \\ 2.3869 & 1.8292 & 1.9630 \\ 2.3869 & 1.8515 & 2.0300 \\ 2.5207 & 1.8961 & 1.9853 \\ 2.5876 & 1.8961 & 1.9853 \end{bmatrix} OCV = \begin{bmatrix} 3.4352 & 3.4355 & 3.4357 \\ 3.5335 & 3.5337 & 3.5338 \\ 3.6120 & 3.6140 & 3.6180 \\ 3.7048 & 3.7049 & 3.7051 \\ 3.8636 & 3.8637 & 3.8637 \\ 4.0390 & 4.0390 & 4.0390 \\ 4.1600 & 4.1600 & 4.1610 \end{bmatrix}$$

Lastly, the advanced virtual-EV generates output battery signals with a sampling frequency of 0.1 seconds that, being smaller than the simplified virtual-EV's, allows the capturing of even tinier signal variations.

IV. The Simulation

The distinct design choices for the simplified and advanced virtual-EVs, as discussed in Section III-B, inevitably lead to results characterized by different precision and accuracy. In Section V, the simulation results from both virtual-EVs are thoroughly confronted.

However, despite the block design differences and the dissimilar temporal granularity of the outputs, the set of inputs and generated outputs for the two simulators remains the same. Indeed, as shown in Figure 5, both simplified and advanced virtual-EVs receive the input DC as a time series of speed measurements, the initial battery's SOC, SOH, internal temperature, and environmental temperature (as a constant or

time series). The virtual-EV's inputs and initial values, for each simulation, are selected sourcing from the corresponding real driving session, attempting to replicate the same internal and environmental conditions.

The generated output time series for the battery pack, instead, include current, voltage, SOC, and internal temperature. These variables are computed and updated at each simulation time step based on the given inputs. The simulation evolves in time according to the input speed time series, which globally describes the driving pattern, hence, the length of the input speed signal determines how long the simulation will last.

Furthermore, the real battery signals are individually resampled using linear interpolation with a time step of 0.2 and 0.1 seconds for the simplified and advanced virtual-EVs' outputs, respectively. In this way, a consistent time base is ensured to objectively compare the simulated and real time series with the proper temporal granularity. During the validation phase of the simulators, 23 simulations are independently executed for both virtual-EVs, matching the available real driving session data described in Table II. The selection of the inputs and the real data resampling procedure ensure consistency between synthetic and reference time series during the validation phase.

The simulations were run over an NVIDIA GeForce RTX 3070 Ti GPU, and Table V reports the execution time for each input DC and for both virtual-EVs, averaged over five simulation instances. Generally, the advanced simulator requires longer execution times than the simplified one, mainly due to its higher temporal granularity of the outputs. The simulation results are discussed in the following Section V, while Section VI provides different application scenarios considering the trade-off between execution times and accuracy of the two virtual-EVs.

TABLE V
THE AVERAGE EXECUTION TIMES, IN SECONDS, FOR EACH SIMULATED DC AND FOR BOTH VIRTUAL-EVS.

| Driving cycle	Simplified virtual-EV [s]	Advanced virtual-EV [s]
DC1	81.90	144.30
DC2	47.01	125.38
DC3	37.24	102.50
DC4	53.09	140.58
DC5	44.15	222.41
DC6	80.90	123.25
DC7	12.12	26.41
DC8	45.04	51.28
DC9	31.04	38.48
DC10	18.01	46.54
DC11	77.21	216.00
DC12	18.95	84.60
DC13	23.86	65.06
DC14	22.45	61.31
DC15	16.95	28.04
DC16	10.88	46.28
DC17	5.06	46.14
DC18	17.05	35.74
DC19	18.47	52.46
DC20	13.46	69.23
DC21	20.83	115.65
DC22	27.39	63.31
DC23	41.48	104.91
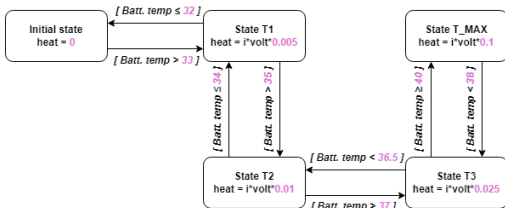
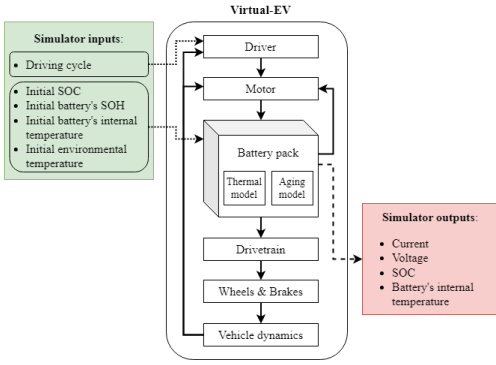Fig. 4. The inner structure of the thermal model state flow chart.

Fig. 5. The general inner structure of the virtual-EV along with its inputs and outputs.

V. Experimental results

In this section, the simulation results obtained by the simplified and advanced virtual-EVs are discussed and compared. The *Root Mean Square Error* (RMSE) and *Coefficient of determination* (R^2) are utilized to measure the deviation between actual and synthetic output signals. The RMSE assesses the average difference between the simulated and actual values, whereas the R^2 measures the proportion of the observed values' variability that can be explained by the predicted values. The performance metrics are defined as follows,

$$RMSE = \sqrt{\frac{\sum_{n=1}^{N}(y_{sim,n} - y_{real,n})^2}{N}} \quad (2)$$

$$R^2 = 1 - \frac{\sum_{n=1}^{N}(y_{real,n} - y_{sim,n})^2}{\sum_{n=1}^{N}(y_{real,n} - \overline{y}_{real})^2} \quad (3)$$

where y_{sim} refers to the simulated value, y_{real} is the actual value, $\overline{y}_{real}$ refers to the mean value of the actual values, and N is the total number of samples. The performances of the two virtual-EVs are independently assessed comparing the synthetic outputs of current, voltage, SOC, and internal temperature with the corresponding real signals, for each driving session in Table II and globally.

Figure 6 shows the simulation outputs of both simplified and advanced virtual-EVs against the actual battery pack's signals, for three driving sessions, namely DC4, DC11, and DC23. Observing the curves in Figure 6, the simulated signals generated by the two virtual-EVs, generally, follow the measured ones, and a precise matching can be observed. Nevertheless, the higher precision of the advanced over the simplified one can be detected observing, for instance, the curves of SOC and temperature, which closely follow the target real signals. Comparing the values of the synthetic voltage curves with those of the target signal, the voltage generated by advanced virtual-EV assumes values closer to those of the target voltage. Regarding the output synthetic current, both virtual-EVs perform similarly, although the advanced simulator remains more accurate.

However, observing Figure 6, the reader can notice a quite remarkable difference, in terms of spikes and variability, between the synthetic currents and voltages and the respective real signals. Indeed, as reported in Table III, the EV speed, utilized as one of the inputs for the two simulators, has

been collected with a sampling frequency of 19 seconds, in contraposition to the 0.1 seconds of current and voltage.

As described in the Section IV, the simulation evolves in time according to the input speed time series, which perforce does not keep all driving variations due to its low sampling frequency. Conversely, the signals of current and voltage include much more information about smaller changes in the real driving behavior. Therefore, the different temporal granularity of the real signals inevitably leads to an approximation of the results, making the synthetic current and voltage curves less informative than the relative real ones. Nevertheless, the virtual-EVs, mainly the advanced one, exhibit good accuracy which stands out when comparing synthetic curves of SOC and internal temperature with the real signals, characterized instead by a lower sampling frequency.

Table VI reports the performances of both simplified and advanced virtual-EVs in terms of RMSE and R^2, respectively, for each driving session, presented in Table II, and globally. Observing Table VI, it is possible to demonstrate the higher accuracy of the advanced virtual-EV which achieves overall lower RMSE and higher R^2 for all output signals, compared to the simplified one. The RMSE reduction for the current and voltage are substantial and systematic, reaching 4.85 A for DC13 and 9.67 V for DC11, respectively. However, the amplest improvement concerns the SOC. In fact, with the advanced virtual-EV, it is possible to reduce the RMSE for the SOC down to a few percentage points, in contraposition to the simplified one. For example, the advanced simulation for DC23 achieves an RMSE and R^2 for the SOC of 1.11% and 1.0, respectively, leading to a reduction of 8.46% for the RMSE and an increase of 0.30 for the R^2 over the simplified simulation. Overall, the advanced simulator reduces the RMSE for current, voltage, SOC, and internal temperature of 0.52 A, 5.23 V, 7.60%, and 0.66°C, respectively.

The simplified virtual-EV outperforms the advanced one, mostly for DC7 and DC8. The explanation for such occurrence lies on the parameterization of the simplified battery pack, discussed in Section III-B2. During such a phase, the error minimization step has been accomplished utilizing real data signals belonging to a driving session taken when the EV's battery pack was characterized by an SOH of 93%. Therefore, the simplified virtual-EV appears to be more precise for DC marked with an SOH closer to 93%. On the contrary, the advanced virtual-EV does not require such a parameterization, which leads to a better adaptability in different environmental and internal conditions for the EV.

To further demonstrate the virtual-EVs' capacity at generalizing over EVs equipped with a battery pack at different aging statuses, the available driving sessions have been clustered by their relative SOH value, and the performance metrics are observed for each aging status alone. Table VII reports the RMSE and R^2 computed, comparing the synthetic curves with the respective real ones for all DCs labeled with the same battery pack's SOH. Despite the low number of available DCs, observing Table VII, the reader can notice the virtual-EVs' capability at generalizing over distinct initial SOH values being the errors somehow comparable. For instance, the advanced virtual-EV achieves an R^2 up to 0.33, 0.92, 0.97, and
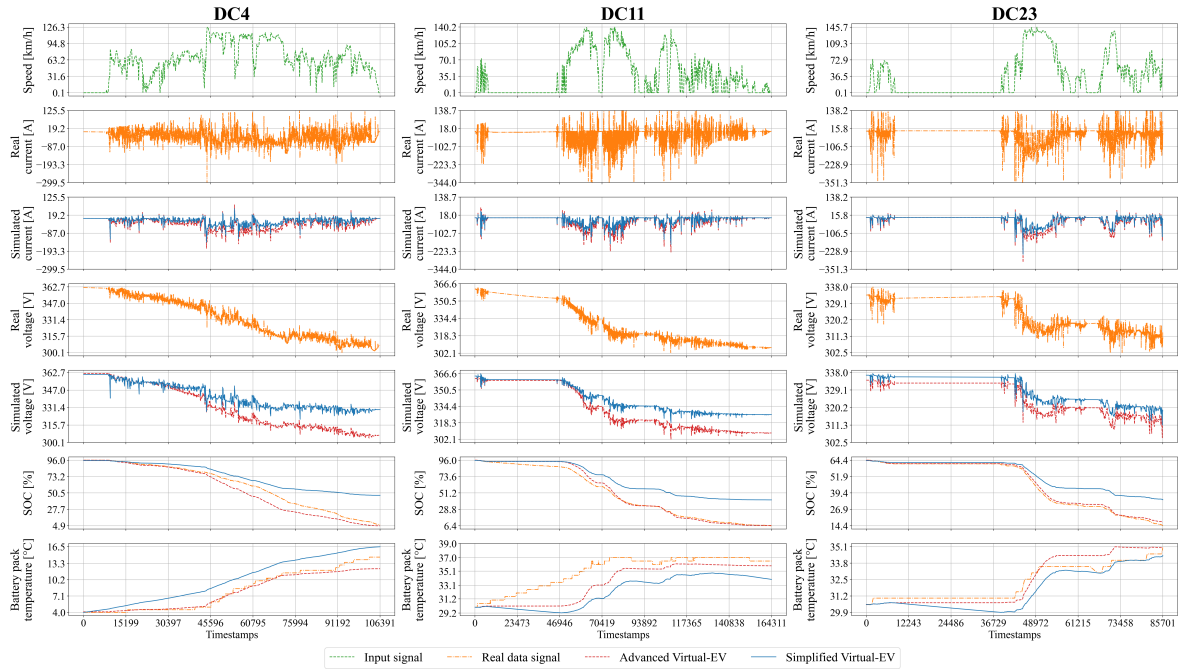
Fig. 6. The comparison between synthetic outputs of current, voltage, SOC, and internal temperature, generated by the simplified and advanced virtual-EVs, and the relative target signals.

TABLE VI
The validation results in terms of RMSE and R^2 achieved by both simplified and advanced virtual-EVs, obtained by comparing the synthetic outputs with the respective target ones.

| Driving cycle | RMSE | | | | | | | | R^2 | | | | | | | |
| | Simplified virtual-EV | | | | Advanced virtual-EV | | | | Simplified virtual-EV | | | | Advanced virtual-EV | | | |
	Current [A]	Voltage [V]	SOC [%]	Battery internal temp. [°C]	Current [A]	Voltage [V]	SOC [%]	Battery internal temp. [°C]	Current	Voltage	SOC	Battery internal temp.	Current	Voltage	SOC	Battery internal temp.
DC1	39.84	9.94	12.2	**1.35**	**38.37**	**5.29**	**7.24**	3.21	0.31	0.34	0.50	**0.89**	**0.36**	**0.81**	**0.82**	0.38
DC2	34.11	7.35	8.62	2.98	**31.92**	**3.40**	**3.48**	**0.93**	0.19	0.12	0.68	0.0	**0.29**	**0.81**	**0.95**	**0.69**
DC3	24.52	4.53	5.00	1.52	**23.67**	**2.30**	**2.08**	**1.27**	0.23	0.33	0.46	0.0	**0.29**	**0.83**	**0.91**	**0.06**
DC4	34.47	12.16	17.65	2.20	**32.91**	**3.69**	**7.88**	**0.74**	0.13	0.61	0.65	0.66	**0.21**	**0.96**	**0.93**	**0.96**
DC5	33.55	6.78	5.18	**1.21**	**33.0**	**4.32**	**3.92**	1.22	0.14	0.54	0.77	**0.44**	**0.17**	**0.81**	**0.87**	0.43
DC6	34.86	13.57	16.64	2.81	**34.38**	**4.63**	**7.36**	**0.43**	0.14	0.0	0.09	0.0	**0.16**	**0.85**	**0.82**	**0.75**
DC7	**47.51**	**5.82**	**3.65**	**1.30**	50.74	7.10	4.93	1.82	0.0	**0.55**	**0.83**	0.0	0.0	0.32	0.69	0.0
DC8	**56.96**	**4.61**	**3.77**	3.59	62.59	5.30	4.77	**1.62**	0.0	**0.57**	**0.95**	0.0	0.0	0.43	0.92	0.0
DC9	**31.08**	7.65	7.31	**0.18**	31.12	**4.75**	**5.71**	0.47	0.29	0.31	0.59	**0.98**	0.29	**0.73**	**0.75**	0.86
DC10	33.72	1.53	3.61	**1.15**	**32.81**	**1.45**	**0.78**	1.37	0.36	0.73	0.57	0.0	**0.40**	**0.75**	**0.98**	0.0
DC11	31.88	13.03	21.77	3.15	**31.68**	**3.36**	**3.79**	**1.97**	0.37	0.55	0.57	0.0	**0.38**	**0.97**	**0.99**	0.23
DC12	48.42	**3.38**	5.06	1.23	**47.9**	3.88	**2.40**	**0.41**	0.0	0.0	0.0	0.0	0.0	0.0	**0.74**	**0.58**
DC13	76.83	12.96	18.79	2.98	**71.98**	**4.12**	**1.77**	**1.73**	0.14	0.38	0.51	0.51	**0.24**	**0.94**	**1.0**	**0.83**
DC14	40.97	5.86	4.84	1.11	**40.94**	**4.27**	**4.59**	**0.56**	0.37	0.60	0.81	0.63	0.37	**0.79**	**0.82**	**0.91**
DC15	35.87	4.43	4.74	**0.36**	**33.28**	**1.97**	**0.36**	0.85	0.31	0.53	0.47	**0.86**	**0.41**	**0.91**	**1.0**	0.20
DC16	41.38	5.51	2.76	0.55	**40.13**	**2.36**	**0.26**	**0.22**	0.26	0.0	0.10	0.0	**0.30**	**0.27**	**0.99**	**0.18**
DC17	18.79	2.63	0.83	0.20	**16.05**	**2.13**	**0.44**	**0.16**	0.24	0.0	0.0	0.0	**0.45**	0.0	**0.32**	0.0
DC18	93.34	8.58	7.02	4.02	**91.92**	**5.74**	**3.2**	**3.73**	0.17	0.21	0.37	0.0	**0.19**	**0.65**	**0.87**	0.0
DC19	96.24	7.78	6.96	4.70	**94.01**	**4.35**	**1.64**	**3.02**	0.37	0.52	0.85	0.0	**0.40**	**0.85**	**0.99**	**0.62**
DC20	**31.27**	5.75	**1.22**	**0.33**	33.54	1.59	4.37	0.38	**0.48**	0.33	**0.97**	**0.80**	0.40	**0.94**	0.61	0.73
DC21	34.26	3.64	2.22	**0.41**	**34.21**	**2.27**	**1.27**	0.70	0.28	0.0	0.04	**0.45**	0.28	**0.55**	**0.69**	0.0
DC22	57.81	7.14	6.42	**3.65**	**57.18**	**2.77**	**1.27**	4.16	0.12	0.0	0.27	0.0	**0.14**	**0.84**	**0.97**	0.0
DC23	40.64	5.96	9.57	**0.76**	**38.43**	**2.28**	**1.11**	**0.65**	0.43	0.53	0.70	0.69	**0.49**	**0.93**	**1.0**	**0.77**
Tot	43.86	9.30	12.44	2.40	**43.34**	**4.07**	**4.84**	**1.74**	0.26	0.65	0.75	0.95	**0.28**	**0.93**	**0.96**	**0.97**

0.98, for current, voltage, and SOC, respectively, across all available SOH values. Similar R^2 ranges can be observed for the simplified virtual-EV. However, the magnitude of the errors is highly related to the DC itself, and the environmental and road conditions are unknown to us. Hence, it is not possible to conduct a complete and fair analysis per battery's SOH. Nonetheless, the errors across DCs clustered by SOH are within comparable ranges, which proves the virtual-EVs to be accurate at simulating different aged battery packs.

VI. Conclusion

In this work, two virtual-EVs have been compared, each generating battery signals, given the input driving cycle, with a different level of precision. The EV's environmental and internal conditions are highly customizable by the user through the selection of inputs of interest. The simulation results achieved by both simplified and advanced virtual-EV are promising, and they demonstrate the effectiveness of the

suggested methodology, allowing the extension of the analysis to, potentially, any EV of interest. Moreover, the modeling of a multi-cell battery pack proved to be beneficial. Indeed, for DCs characterized by a battery's SOH spanning from 85% to 99%, the advanced virtual-EV achieves an RMSE lower than 6 V and an R^2 generally higher than 0.90 for the voltage; while, for the SOC, the RMSE does not exceed 7%.

Nonetheless, the two virtual-EVs might be utilized for distinct applications, considering their distinctive computational burden and precision. Indeed, the simplified EV simulator is generally more than twice as fast as the advanced simulator. Therefore, the user could employ the simplified virtual-EV to simulate EVs, seen as floating batteries in a collective smart grid scenario, fastening the retrieval of the results with a lower precision. Conversely, the advanced virtual-EV could be utilized to simulate, at low-level, individual EVs collecting more accurate outputs at the expense of faster data retrieval, allowing, for instance, the development of machine learning

TABLE VII
THE VALIDATION RESULTS IN TERMS OF RMSE AND R^2 ACHIEVED BY BOTH SIMPLIFIED AND ADVANCED VIRTUAL-EVS, OBTAINED BY COMPARING THE SYNTHETIC OUTPUTS WITH THE RESPECTIVE TARGET ONES GROUPING DCS WITH THE SAME BATTERY PACK'S SOH.

| | | RMSE | | | | | | | | R^2 | | | | | | | |
| | | Simple virtual-EV | | | | Advanced virtual-EV | | | | Simple virtual-EV | | | | Advanced virtual-EV | | | |
SOH [%]	# available DCs	Current [A]	Voltage [V]	SOC [%]	Battery internal temp. [°C]	Current [A]	Voltage [V]	SOC [%]	Battery internal temp. [°C]	Current	Voltage	SOC	Battery internal temp.	Current	Voltage	SOC	Battery internal temp.
85	3	34.23	7.88	9.46	**2.08**	**32.67**	**4.02**	**5.05**	2.17	0.27	0.65	0.78	**0.46**	**0.33**	**0.91**	**0.94**	0.41
88	3	34.43	11.81	15.0	2.33	**33.62**	**4.30**	**6.85**	**0.78**	0.18	0.39	0.54	0.69	**0.22**	**0.92**	**0.90**	**0.96**
92	2	**53.73**	**5.08**	**3.73**	2.97	58.57	6.01	4.83	**1.69**	0.0	**0.91**	**0.98**	0.0	0.0	0.87	0.97	**0.27**
93	3	31.87	11.24	18.07	2.58	**31.66**	**3.63**	**4.18**	**1.67**	0.36	0.60	0.66	0.80	**0.37**	**0.96**	**0.98**	**0.92**
94	3	58.66	8.81	12.12	2.04	**56.19**	**4.11**	**3.17**	**1.13**	0.25	0.69	0.78	0.93	**0.31**	**0.93**	**0.98**	**0.98**
95	3	36.94	4.72	4.04	**0.42**	**34.86**	**2.11**	**0.34**	0.68	0.29	0.87	0.95	**0.99**	**0.37**	**0.97**	**1.0**	0.96
96	2	94.80	8.19	6.99	4.37	**92.97**	**5.09**	**2.54**	**3.39**	0.30	0.72	0.90	0.61	**0.33**	**0.89**	**0.99**	0.77
98	1	**31.27**	5.25	**1.22**	**0.33**	33.54	**1.59**	4.37	0.38	**0.48**	0.33	**0.97**	**0.80**	0.40	**0.94**	0.61	0.73
99	3	45.19	5.95	7.69	**2.04**	**43.96**	**2.43**	**1.19**	2.31	0.30	0.85	0.89	**0.83**	**0.34**	**0.97**	**1.0**	0.78

models to estimate the battery pack's SOH.

The future works include: investigating the current offset contribution in relation to the EV's aging status, and extending it to the simplified virtual-EV; ii) embedding the virtual-EVs in a wider co-simulation platform, extracting customizable driving sessions retrieving more information about the road conditions and slope, making the results even more accurate and allowing the generation of a wide, real, and synthetic EV's battery pack dataset.

REFERENCES

[1] IEA, "Greenhouse gas emissions from energy data explorer," 2021. [Online]. Available: https://www.iea.org/data-and-statistics/data-tools/greenhouse-gas-emissions-from-energy-data-explorer

[2] EEA, *Decarbonising road transport : the role of vehicles, fuels and transport demand*. Publications Office of the European Union, 2022.

[3] G. dos Reis, C. Strange, M. Yadav, and S. Li, "Lithium-ion battery data and where to find it," *Energy and AI*, vol. 5, p. 100081, 2021.

[4] L. H. Saw, Y. Ye, and A. A. Tay, "Integration issues of lithium-ion battery into electric vehicles battery pack," *Journal of Cleaner Production*, vol. 113, pp. 1032–1045, 2016.

[5] M. Ziegler and J. Trancik, "Re-examining rates of lithium-ion battery technology improvement and cost decline," *Energy & Environmental Science*, vol. 14, Apr. 2021.

[6] P. Jones, U. Stimming, and A. Lee, "Impedance-based forecasting of lithium-ion battery performance amid uneven usage," *Nature Communications*, vol. 13, Aug. 2022.

[7] J. Zhao, H. Ling, J. Wang, A. F. Burke, and Y. Lian, "Data-driven prediction of battery failure for electric vehicles," *iScience*, vol. 25, no. 4, p. 104172, 2022.

[8] C. Birkl, "Oxford battery degradation dataset 1," 2017.

[9] B. Saha and K. Goebel, "Battery data set. NASA ames progn res center," 2007.

[10] X. Yuan, C. Zhang, G. Hong, X. Huang, and L. Li, "Method for evaluating the real-world driving energy consumptions of electric vehicles," *Energy*, vol. 141, pp. 1955–1968, 2017.

[11] R. Gallo, A. Aliberti, E. Patti, T. Monopoli, M. Zampolli, R. Jaboeuf, and T. Paolo, "Modelling battery packs of real-world electric vehicles from data sheet information," in *2023 IEEE International Conference on Environment and Electrical Engineering and 2023 IEEE Industrial and Commercial Power Systems Europe (EEEIC / I&CPS Europe)*, 2023, pp. 1–6.

[12] R. Gallo, A. Aliberti, E. Patti, G. Bussolo, M. Zampolli, R. Jaboeuf, and T. Paolo, "An electric vehicle simulator for realistic battery signals generation from data-sheet and real-world data," in *2023 IEEE 47th Annual Computers, Software, and Applications Conference (COMPSAC)*, 2023, pp. 1501–1506.

[13] B. Canizes, J. Soares, A. Costa, T. Pinto, F. Lezama, P. Novais, and Z. Vale, "Electric vehicles' user charging behaviour simulator for a smart city," *Energies*, vol. 12, no. 8, 2019.

[14] E. S. Rigas, S. Karapostolakis, N. Bassiliades, and S. D. Ramchurn, "Evlibsim: A tool for the simulation of electric vehicles' charging stations using the evlib library," *Simulation Modelling Practice and Theory*, vol. 87, pp. 99–119, 2018.

[15] C. Gaete-Morales, H. Kramer, W.-P. Schill, and A. Zerrahn, "An open tool for creating battery-electric vehicle time series from empirical data, emobpy," *Scientific Data*, vol. 8, no. 1, June 2021.

[16] L. Ciabattoni, S. Cardarelli, M. D. Somma, G. Graditi, and G. Comodi, "A novel open-source simulator of electric vehicles in a demand-side management scenario," *Energies*, vol. 14, no. 6, 2021.

[17] C. Baker, M. Moniot, A. Brooker, L. Wang, E. Wood, and J. Gonder, "Future automotive systems technology simulator (fastsim) validation report - 2021," Oct. 2021.

[18] S. Lee, B. Lee, J. McDonald, and E. Nam, "Modeling and validation of lithium-ion automotive battery packs," 04 2013.

[19] R. Hanifah, S. Toha, and S. Ahmad, "Electric vehicle battery modelling and performance comparison in relation to range anxiety," *Procedia Computer Science*, vol. 76, pp. 250–256, 2015, 2015 IEEE International Symposium on Robotics and Intelligent Sensors (IEEE IRIS2015). [Online]. Available: https://www.sciencedirect.com/science/article/pii/S187705091503851X

[20] I. Baboselac, Z. Hederić, and T. Bensic, "Matlab simulation model for dynamic mode of the lithium-ion batteries to power the ev," *Technical Journal*, vol. 11, pp. 7–13, 01 2017.

[21] R. C. Kroeze and P. T. Krein, "Electrical battery model for use in dynamic electric vehicle simulations," in *2008 IEEE Power Electronics Specialists Conference*, 2008, pp. 1336–1342.

[22] D. Qin, J. Li, T. Wang, and D. Zhang, "Modeling and simulating a battery for an electric vehicle based on modelica," *Automotive Innovation*, vol. 2, no. 3, pp. 169–177, Sep 2019. [Online]. Available: https://doi.org/10.1007/s42154-019-00066-0

[23] D. Simic and T. Bäuml, "Implementation of hybrid electric vehicles using the vehicleinterfaces and the smartelectricdrives libraries," Jan. 2008.

[24] J. Shin, W. Kim, K. Yoo, H. Kim, and M. Han, "Vehicular level battery modeling and its application to battery electric vehicle simulation," *Journal of Power Sources*, vol. 556, p. 232531, 2023. [Online]. Available: https://www.sciencedirect.com/science/article/pii/S0378775322015087

[25] MathWorks., "Transmission and drivetrain," 2023. [Online]. Available: https://it.mathworks.com/help/autoblks/transmission-and-drivetrain.html

[26] ——, "Open differential," 2023. [Online]. Available: https://it.mathworks.com/help/autoblks/ref/opendifferential.html

[27] ——, "Mapped motor simulink block," 2023. [Online]. Available: https://it.mathworks.com/help/autoblks/ref/mappedmotor.html

[28] ——, "Documentation simscape," 2023. [Online]. Available: https://it.mathworks.com/products/simscape.html

[29] ——, "Vehicle body 1dof longitudinal," 2023. [Online]. Available: https://it.mathworks.com/help/autoblks/ref/vehiclebody1doflongitudinal.html

[30] ——, "Vehicle body 3dof longitudinal," 2023. [Online]. Available: https://www.mathworks.com/help/vdynblks/ref/vehiclebody3doflongitudinal.html

[31] ——, "Generic battery model," 2023. [Online]. Available: https://it.mathworks.com/help/sps/powersys/ref/battery.html

[32] ——, "Simscape battery," 2023. [Online]. Available: https://it.mathworks.com/products/ simscape-battery.html

[33] ——, "System level simulation technique for optimizing battery thermal management system of ev," 2023. [Online]. Available: https://it.mathworks.com/content/ dam/mathworks/mathworks-dot-com/images/events/matlabexpo/in/ 2020/system-level-simulation-technique-for-optimizing-batterythermal- management-system-of-ev.pdf

[34] M. Zwicker, M. Moghadam, W. Zhang, and C. Nielsen, "Automotive battery pack manufacturing – a review of battery to tab joining," *Journal of Advanced Joining Processes*, vol. 1, p. 100017, 2020. [Online]. Available: https://www.sciencedirect.com/science/article/pii/S2666330920300157

[35] MathWorks Student Competitions Team, "Battery (table-based)," 2023. [Online]. Available: https://www.mathworks.com/help/simscape-battery/ref/batterytablebased.html